International Journal of Nanomedicine

Dovepress

open access to scientific and medical research

Open Access Full Text Article

ORIGINAL RESEARCH

Hollow CeO_2 with ROS-Scavenging Activity to Alleviate Colitis in Mice

Jing Yang[1,*]
Jinzhe Zhou[2,*]
Yingying Zhao[1]
Liangchen Zhu[2]
Guanghong Luo[3]
BuJun Ge[2]

[1]Department of Gastroenterology, The First Affiliated Hospital of Shandong First Medical University & Shandong Provincial Qianfoshan Hospital, Jinan, People's Republic of China; [2]Department of General Surgery, Tongji Hospital, Tongji University School of Medicine, Shanghai, People's Republic of China; [3]Department of Radiation Oncology, Shenzhen People's Hospital (The Second Clinical Medical College, Jinan University, The First Affiliated Hospital, Southern University of Science and Technology), Shenzhen, People's Republic of China

*These authors contributed equally to this work

Introduction: Excessive production of reactive oxygen species (ROS) to induce high oxidative stress is one of the main causes of colitis; thus, it has been regarded as a therapeutic target for colitis treatment. And the nanomaterial-based therapeutic strategies are effective against colitis. However, the previous elaborately designed materials exhibit limited application due to the uncertain biocompatibility and complicated manufacturing processes.

Methods: In this study, the highly monodisperse hollow CeO_2 nanoparticles (H-CeO_2) with uniform morphology were obtained by in situ growing CeO_2 on solid silica nanoparticles and subsequently removing the silica core. The H-CeO_2 was further modified with PEG, which owned excellent biological stability and biocompatibility. The experimental model of colitis induced by dextran sulfate sodium (DSS) was used to investigate the anti-inflammatory effect of H-CeO_2-PEG.

Results: The H-CeO_2-PEG showed good ROS scavenging efficacy and decreased the levels of proinflammatory cytokines (IL-6, IL-1β, IL-18, and TNF-α) in DSS-induced colitis mice. Furthermore, H-CeO_2-PEG inhibited the activation of the MAPK signalling pathway to alleviate colitis.

Conclusion: This study reveals the therapeutic effects of CeO_2-based nanomedicine toward colitis and elucidates the specific signalling pathway involved, which provides potential alternative therapeutic options for patients with inflammation tissue.

Keywords: hollow CeO_2, ROS, inflammation, colitis, MAPK signalling pathway

Introduction

Inflammation, a critical defensive response to foreign pathogens that is regulated by the innate and adaptive immune systems,[1] is related to abnormal biological processes, disorder-related diseases and different cancers,[2,3] and divided into acute inflammation and chronic inflammation. Acute inflammation leads to serious exudative lesions, and chronic inflammation is known to promote and exacerbate malignancy.[4] Colitis is an inflammatory condition of the colon caused by a variety of factors.[5–7] The production of various reactive oxygen species (ROS), including hydrogen peroxide (H_2O_2), nitric oxide (NO), hydroxyl radicals ($^{\bullet}OH$) and superoxide anions ($^{\bullet}OOH$), is vital for the progression of colitis.[8–10] ROS are necessary for the mediation of inflammation and signalling molecules to regulate the immune response, which are generated from different biomolecules via many cascade reactions and act as strong oxidants that induce damage to proteins, lipids, and DNA and other biomacromolecules or act as mediators to regulate the expression of downstream genes.[11,12] Thus, the ROS have been proposed as an effective target for colitis treatment.[13–15]

Correspondence: Guanghong Luo; Bujun Ge
Email luo.guanghong@szhospital.com; gbj109@126.com

Received: 13 May 2021
Accepted: 22 September 2021
Published: 8 October 2021

In recent years, with the development of nanomedicine, many nanomaterials have been explored and synthesised for various diseases' treatment.[16–18] Nanomaterials own reductive properties and the ability to regulate cellular homeostasis could be applied for improving the targeting capability and reducing side effects. Thus, the nanomaterials show huge potential in the treatment of colitis compared to traditional drugs.[19,20] For instance, molecular hydrogen can specifically scavenge highly cytotoxic ROS, including $^{\bullet}OH$ and $ONOO^{-}$, and preserve other necessary ROS for normal signalling pathway to exert simultaneous antioxidative and anti-inflammatory effects.[21] In a study, Chen and colleagues constructed a Polyvinylpyrrolidone (PVP)-coated Prussian blue nanoparticles with a size of 50 nm by one-pot strategy, which exhibited good physiological stability and biosafety, and showed to be multienzyme mimetics that scavenge ROS via multienzyme-like activity, including peroxidase (POD), catalase (CAT), and superoxide dismutase (SOD)-like activity and inhibited the generation of proinflammatory cytokine significantly to reduce colitis effectively.[22] Except for the novel nanoparticle mentioned above, many other familiar nanomaterials have also been applied to the treatment of colitis. Abdelmegid Amira M et al revealed that gold nanoparticles can induce an increase in the expression of IL-17 to have a therapeutic effect on dextran sulfate sodium (DSS)-induced UC in mice,[23] and Wu's group study revealed that PtNPs upregulate the heat-shock protein 25 and tight junction proteins, which enhances the gut-barrier function, and PtNPs attenuate the colonic inflammation by decreasing the colonic and peripheral levels of interleukin-6 and tumor necrosis factor-α, and peripheral counts of white blood cells; and also suppressing the production of proinflammatory mediators, thus PtNPs exerted direct anti-inflammatory activities.[24] In other studies, Ruiz Pedro A et al reported that titanium dioxide (TiO_2) nanomaterials are capable to trigger the release of NLRP3-associated IL-1β and IL-18 inflammasomes, leading to decreased production of ROS and enhanced epithelial permeability of IEC monolayers to exacerbate DSS-induced colitis.[25] Akihiro Nishiguchi and Tetsushi Taguchi construct an anti-inflammatory and biocompatible compound constitute polyamine and branched oligoethyleneimine (bOEI); moreover, the bOEI-300 strongly suppresses the secretion of pro-inflammatory cytokines from macrophages by scavenging reactive oxygen species and inhibit the nuclear translocation of the nuclear factor kappa-B, thus it enhances the therapeutic efficacy of inflammatory diseases.[26] Thus, the application of nanoparticles that eliminate ROS at the site of inflammation is an attractive and urgently needed strategy for colitis therapy.

Recently, Cerium (IV) oxides with the chemical formula CeO_2 and belonging to lanthanide metal oxide, nanoparticles (CeO_2) have gained increasing attention due to their anti-inflammatory and antioxidant properties, immune regulation ability, high cytocompatibility and low cytotoxicity and their application in inflammatory-associated diseases.[18,27–31] Studies have shown that CeO_2 owns favourable therapeutic effects by effectively eliminating ROS, specifically $^{\bullet}OH$, H_2O_2, and $^{\bullet}OOH$, and its enzyme-like activities, including CAT, POD, and SOD-like activities, thus inducing alterations in intracellular oxygen content and regulating the redox status.[32–34] Hui Wei et al, build a CeO_2@Montmorillonite nanozyme for orally administering inflammatory bowel disease therapy, where the CeO_2 exhibits superoxide dismutase- and catalase-like activities, and hydroxyl radical scavenging activity that could efficiently scavenge ROS, and the negatively charged montmorillonite can be specifically adsorbed onto positively charged inflamed colon tissue via electrostatic interactions for targeted delivery, which reduces inflammation obviously without any significant toxicity after systemic exposure in vivo.[35] Thus, CeO_2 possesses great potential to treat inflammation by targeting ROS scavenging.

Encouraging from previous studies, we synthesized uniform and monodisperse hollow CeO_2 nanoparticles (H-CeO_2) using a hard template strategy and modified them with NH_2-PEG-NH_2 for the treatment of colitis (Figure 1A). H-CeO_2-PEG exhibits excellent stability and biocompatibility. H-CeO_2-PEG can serve as an artificial nanozyme to scavenge ROS to alleviate DSS-induced colitis in mice and inhibit proinflammatory cytokine generation (Figure 1B). Exploration of the molecular mechanism revealed that H-CeO_2-PEG can alleviate inflammation via the ERK1/2/JNK/P38/c-Jun signalling pathways. Moreover, the H-CeO_2-PEG showed excellent biosafety after in vivo systematic exploration. This work provides direct evidence that CeO_2 nanozymes are potential therapeutic nanomedicines for colitis.

Methods

Materials

Tetraethyl orthosilicate (TEOS), poly (allylamine hydrochloride) (PAH), and polyacrylic acid (PAA) were purchased from Sigma-Aldrich (St. Louis, MO, USA). Cerous nitrate

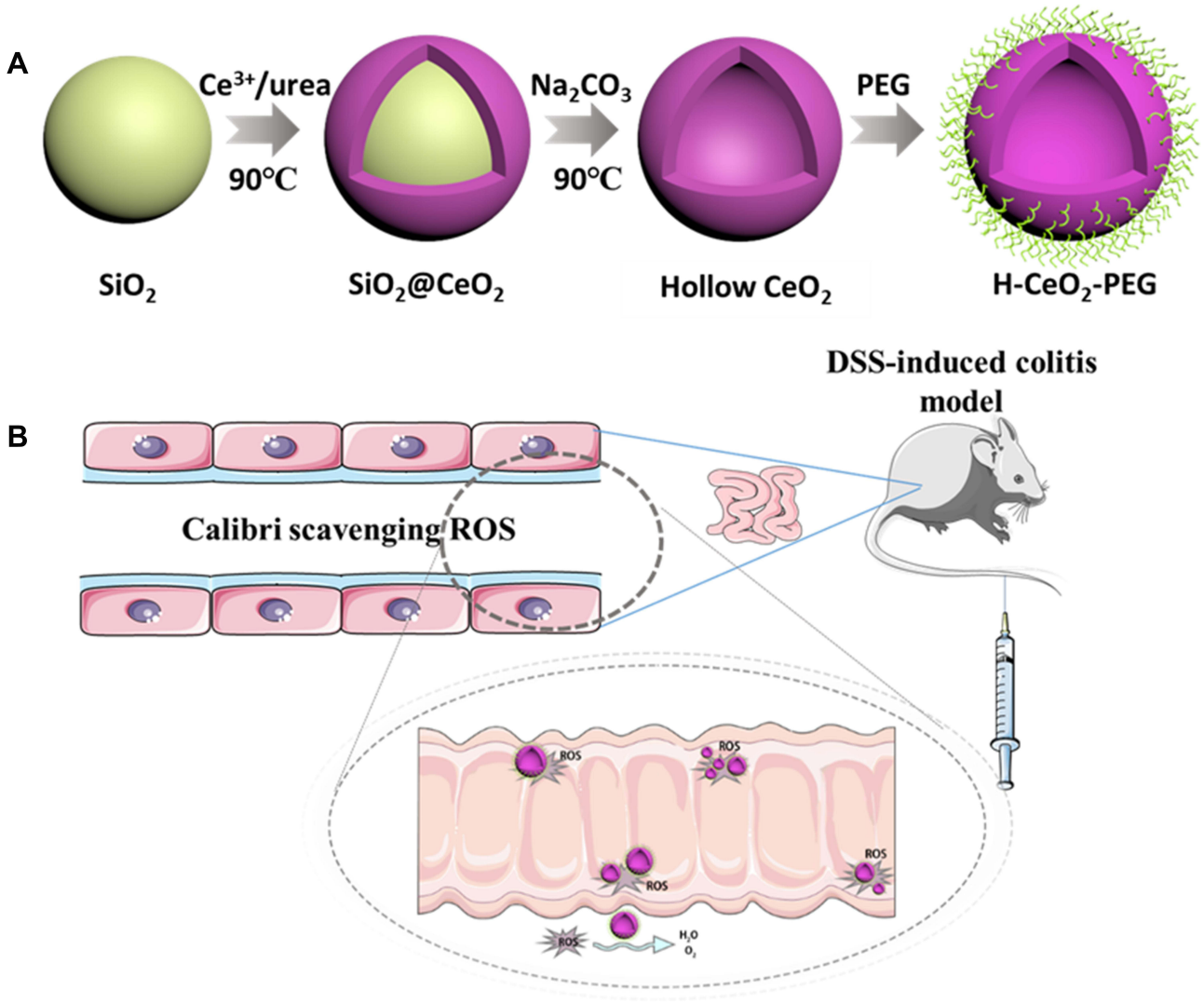

Figure 1 (**A**) Graphical representation of the preparation procedure of H-CeO_2-PEG composites. (**B**) Schematic illustration of the effect of H-CeO_2-PEG on DSS-induced colitis in mice.

($Ce(NO_3)_3$•$6H_2O$), hexamethylenetetramine, hydrogen peroxide solution (H_2O_2, 30%) and sodium hydroxide (NaOH) were obtained from Sinopharm Chemical Reagent CO., Ltd. (China). NH_2-PEG-NH_2 and dextran sulfate sodium salt (DSS) were purchased from Aladdin Reagents (China).

Synthesis of H-CeO_2-PEG

SiO_2 nanoparticles were synthesized by the modified Stöber method as in previous studies.[18] First, a mixture of 35 mL of ethanol, 5 mL of deionized water and 0.6 mL of aqueous ammonia was prepared. Then, 3 mL of TEOS was added to the solution under vigorous stirring. After 12 h, the products were collected by centrifugation and washed with water and ethanol. The as-made SiO_2 nanoparticles were dried in vacuum at 45 °C for 12 h. For the synthesis of hollow CeO_2, 100 mg silica nanoparticles, 0.2 g $Ce(NO_3)_3$•$6H_2O$ and 0.09 g hexamethylenetetramine were dispersed in 50 mL deionized water. The mixture was stirred for 3 h at 90 °C in an oil bath. The product was collected by centrifugation and washed with water and ethanol. The products were calcined at 600 °C for 2 h. The silica core was removed by using 0.5 M NaOH. Finally, H-CeO_2 nanoparticles were obtained after centrifugation and resuspended in aqueous solution. For surface modification of H-CeO_2, 20 mg of H-CeO_2 was dispersed in 40 mL of deionized water, into which 10 mg of PAH was added, and the mixture was stirred for 2 h. Then, H-CeO_2-PAH was collected by centrifugation and washed with water. Similarly, as-made H-CeO_2-PAH was dispersed in 30 mL of water containing 10 mg of PAA and reacted for 2

h. H-CeO_2-PAH/PAA was obtained by centrifugation and washed with ddH_2O. It was further dispersed in 20 mL of water containing 5.6 mg EDC and 4.2 mg of NHS and stirred at room temperature (rt) for 3 h. Then, 10 mg NH_2-PEG-NH_2 was added to the solution under stirring. After 24 h, the prepared H-CeO_2-PEG was obtained by centrifugation and washed with water three times.

Characterization of H-CeO_2-PEG

Transmission electron microscopy (TEM) was performed, and element mapping images were taken with a Tecnai G2 F20 S-Twin TEM at an accelerating voltage of 300 kV. The size and surface potential were measured with photon correlation spectroscopy (Zetasizer Nano ZS, Malvern Instruments Ltd., U.K.), and X-ray diffraction (XRD) was performed with an X-ray diffractometer (Bruker, Germany, Voltage ≤40 kV, 10°≤2 Theta ≤80°). Fourier transform infrared spectroscopy (FTIR) was conducted on an MDTC-EQ-M13-01 instrument (Thermo Scientific, 400 cm^{-1} ≤ wavelength ≤4000 cm^{-1}). UV-vis-NIR absorption spectra were collected with a Hitachi U-3900 with QS-grade quartz cuvettes at rt.

Peroxidase (POD)-Like Activity Assay

The POD-like activity of H-CeO_2-PEG was examined at rt using 3,5,3′,5′-tetramethylbenzidine (TMB) as the detection substrate in 0.2 M HAc-NaAc buffer solution with H_2O_2. The absorbance of the product at 650 nm was measured with a microplate reader (Multiskan Sky Microplate Spectrophotometer, Life). The reaction system contained 30% H_2O_2, 10 mg/mL TMB, 10 μg/mL H-CeO_2-PEG solution, and buffer solution.

Measurement of the Effect of H-CeO_2-PEG on H_2O_2 in vitro

First, 0.6 mL of H_2O_2 solution (0.6 M) in PBS (pH 7.4) and 0.2 mL H-CeO_2-PEG solution (100 μg/mL) were mixed. The oxygen produced was measured with a specific oxygen electrode on a Multiparameter analyser (DZS708, Cany).

Assessment of the Effect of H-CeO_2-PEG on Hydroxyl Radicals

Different concentrations of H-CeO_2-PEG were added to a 0.1 mg/mL TiO_2 (Aladdin Reagents, Shanghai, China) and 50 mM BMPO solution, which was then placed in quartz capillary tubes and exposed to UV light at 300 nm for 10 min. Electron spin resonance (ESR) spectra were recorded with a Bruker EMX spectrometer.

Assessment of the Effect of H-CeO_2-PEG on Superoxide Anions

A xanthine/xanthine oxidase system was applied as the substrate for generating superoxide anions, and BMPO was applied as the superoxide anion detecting agent. Different concentrations of H-CeO_2-PEG were added to the xanthine/xanthine oxidase system for a certain period of time, and ESR spectra were obtained.

In vitro Cell-Killing Experiment

To assess the cytotoxicity of H-CeO_2-PEG, NCM-460, HCT116, and SW480 cells, purchased from ATCC (Manassas, VA, USA), were cultured in 96-well plates at an initial density of 5×10^3 cells/well for 12 h. Next, the different concentrations of H-CeO_2-PEG (0, 5, 10, 25, 50, 100, and 125 μg/mL) were added to the wells. After another 24 or 48 h, the cells were washed with PBS and subjected to standard CCK-8 assay. The absorbance of the solution in each well at 450 nm was measured.

Animal Experiments

BALB/c mice (8–10 weeks, SPF level, 22–25 g, male, n = 30) were obtained from Jake Biotechnology Co., Ltd. (Shanghai, China) and raised in a specific, pathogen-free facility. The mouse experiments performed in this study were approved by the Experimental Animal Committee of Tongji Hospital Tongji University School of Medicine and conducted in accordance with the guidelines of the Tongji Hospital Tongji University School of Medicine. The mice were randomly divided into 3 groups: the control, DSS-induced colitis, and H-CeO_2-PEG DSS-induced colitis groups. The DSS-induced colitis mouse model was constructed by giving mice a 3% (wt%) solution of DSS for drinking instead of water for 1 week. PBS and H-CeO_2-PEG (20 mg/kg) were injected intravenously into DSS-induced colitis mice in the colitis and treatment groups, respectively, on days 1, 3, 5 and 7. During treatment, the body weight of each mouse was determined. On day 21, all mice were anaesthetized using isoflurane, and the disease activity index (DAI) was measured. Whole blood was collected from the eyeballs of mice for serum biochemistry analysis and routine blood index determination, and the main organs (heart, kidney, spleen, and liver) were collected for histological analysis to evaluate biosafety. The

length of the colon was measured, and the colons were washed using saline solution.

Reverse Transcription PCR (qPCR)

Total RNA was isolated from the colonic tissues of control, DSS-induced colitis, and H-CeO_2-PEG-treated DSS-induced colitis mice with TRIzol (Sigma). A First-Strand cDNA Synthesis Kit (APExBIO, Houston, USA) was used to carry out reverse transcription. qPCR analysis was carried out using the QIAGEN OneStep RT-PCR kit (QIAGEN, Germany) on an Applied Biosystems 7500 instrument (Thermo Fisher Scientific, Inc., Waltham, MA, USA). The experiments were performed at least three times. Relative gene expression was calculated by the $2^{-\Delta\Delta CT}$ method.

The Quantification of Cytokines

After the mice were treated at default time, the IBD tissues were collected and lysed with RIPA lysis buffer, and the supernatant was next centrifuged at 12,000 rpm for 20 min at 4 °C, the concentration of protein was measured with BCA Protein Assay Kit, and the content of cytokines (including TNF-α, IL-6, IL-18, and IL-1β) was quantified by commercial kit under the manual instruction.

Cellular Uptake Assay

CLSM were applied to determine cellular uptake efficiency. In brief, 2×10^5 cells/mL HCT116 cells were cultured on 24-well plates with the addition of FITC-H-CeO_2-PEG (5 μg/mL). After 15 min, 1 h or 2 h incubation, the cells were further fixed with 4% paraformaldehyde for 30 min, then stained with DAPI and rinsed with PBS twice. The distribution of H-CeO_2-PEG in the inner cell was examined by a confocal laser scanning microscopy (Leica, Germany).

ROS Detected Assays

To detect the elimination effect of H-CeO_2-PEG on the ROS generated, we used H_2O_2 to induce excessive ROS production in HCT116 cells. In brief, we plated 1×10^5 cells/well in 6-well dishes and treated 100 μM H_2O_2. After 2 h H_2O_2 treatment, 5 μg/mL H-CeO_2-PEG was added for additional 2 h, and the living cells stained 10 μM DCFH-DA (Sigma-Aldrich) and incubated in 37 °C for 15 min. Stained cells were observed using a laser confocal microscope (Leica, Wetzlar, Germany).

Western Blotting Analysis

Colonic tissues from control, DSS-induced colitis, and H-CeO_2-PEG-treated DSS-induced colitis mice were lysed using RIPA buffer (Thermo Fisher Scientific), and the protein concentration was measured using the BCA protein assay kit (Sigma). One microgram of protein was loaded onto 10% SDS-PAGE gels and then transferred to PVDF membranes (Roche, Basel, Switzerland). After blocking in 5% skim milk at rt for 60 min, the membranes were incubated with primary antibodies against ERK (ab184699), pERK (ab201015), JNK (ab179461), pJNK (ab76572), p38 (ab170099), pp38 (ab195049), c-Jun (ab126591), pc-Jun (ab32385), Claudin-1 (ab180158), ZO1 (ab276131), Occu (ab167161), ZO2 (ab191133), and β-Actin (ab8226) overnight at 4 °C and then incubated with secondary antibody (goat anti-rabbit IgG H&L (HRP); ab205718) for 1 h. All antibodies were used at a 1:1000 dilution and were obtained from Abcam. The immunoblots were visualized with an ECL detection system (GE Healthcare, Chicago, IL, USA), and luminescence images were taken with a computer and analysed with ImageJ software (NIH, Bethesda, USA).

Statistical Analysis

All data are presented as the mean ± standard error. Two group comparisons were analysed by unpaired Student's *t*-test. Comparison among multiple groups with one main factor was performed by one-way (ANOVA) followed by a new multiple range test. Statistical calculations were performed using SPSS 19.0 software (*p< 0.05, **p<0.01, ***p<0.001).

Results and Discussion

Synthesis and Characterization of H-CeO_2-PEG

The synthetic procedure of the modified Stöber method[18] for the designed H-CeO_2-PEG is shown in Figure 1A. In brief, CeO_2 was in situ deposited onto solid SiO_2 nanoparticles, which was then etched to obtain hollow structured CeO_2 nanoparticles (NPs). TEM was employed to examine the morphology of nanoparticles. As shown in Figure 2A, the as-prepared solid SiO_2 nanoparticles displayed uniform and monodispersed morphology. After the inner SiO_2 was etched under alkaline condition, the hollow cavity of the obtained H-CeO_2 maintained well without any collapse (Figure 2B). And the elemental mapping images displayed that Ce, O, and Si elements were

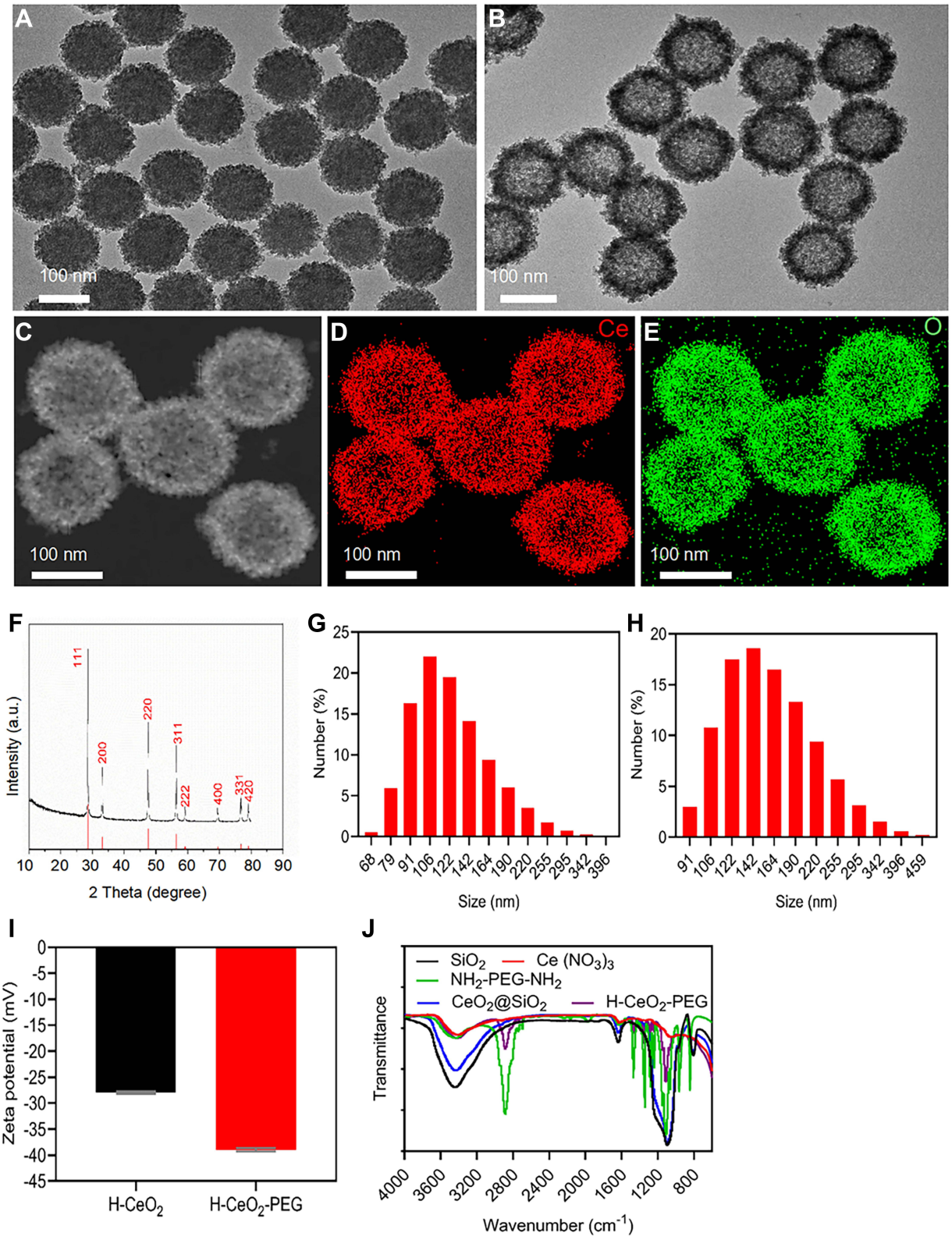

Figure 2 Characterization of H-CeO_2-PEG. TEM images of (**A**) SiO_2@CeO_2 nanoparticles and (**B**) H-CeO_2 nanoparticles. (**C**) Scanning transmission electron microscopy (STEM) image and corresponding element mapping of the H-CeO_2 nanoparticles (**D** and **E**). (**F**) XRD pattern of CeO_2 (ICSD Patterns card no. 43–1002). (**G** and **H**) The size of H-CeO_2 and H-CeO_2-PEG. (**I**) Zeta potential of H-CeO_2 and H-CeO_2-PEG in water. (**J**) FTIR spectrum of PEGylated H-CeO_2.

homogeneously distributed in the shell of H-CeO_2 (Figure 2C–E). Furthermore, the structure of H-CeO_2 NPs was also characterized using XRD. Eight diffraction peaks were observed from the XRD pattern, including eight typical diffraction peaks indexed to the (111), (200), (220), (311), (222), (400), (331) and (420) facets, revealing the presence of CeO_2 crystals (ICSD Patterns card no. 43–1002, Figure 2F). Thus, the above results demonstrated that the versatile CeO_2 fabrication by our methods. The average size as-prepared CeO_2 NPs using dynamic light scattering (DLS) assay was estimated to be 181.8 nm (Figure 2G). And the zeta potential of as-prepared CeO_2 NPs was −27.7 mV (Figure 2I). Then, the polyelectrolyte poly (allylamine hydrochloride) (PAH) and poly (acrylic acid) (PAA) were subsequently coated onto a negative surface of H-CeO_2 by the electrostatic assembly. The carboxyl groups on PAA were utilized to conjugate amine-poly (ethylene glycol) (NH_2-PEG-NH_2). The results of FTIR showed in Figure 2J indicated that the successful PEGylation and PAH/PAA modification of H-CeO_2. Meanwhile, the PEGylation also induced the size and zeta potential of H-CeO_2. As shown in Figures 2H and I, the average size was estimated to be 223 nm, which showed a slight increase of NPs size, and the zeta potential was altered from −27.7 mV to −39.1 mV, suggesting that the colloidal stability of CeO_2 NPs was enhanced with PEGylation. Taking the properties of NH_2-PEG-NH_2 into consideration, the obtained H-CeO_2-PEG in this study could be applied for more efficient drug delivery.

Stability and Cytotoxicity of H-CeO_2-PEG

We first applied UV-Vis spectrum to examine the absorption across the UV to near-infrared region, interestingly, there was no absorption when H-CeO_2-PEG dispersed in ddH_2O (Figure 3A), which might be attributed to the H-CeO_2-PEG dispersed in ddH_2O was transparent. Importantly, the H-CeO_2-PEG NPs showed excellent stability in various solutions, including ddH_2O, PBS, ethanol and DMEM culture (Figures 3B and C). Moreover, the colloidal stability was also identified by DLS analysis, the results showed that the size of H-CeO_2-PEG after dispersed in ddH_2O for 7 days was estimated to be 219.6 nm, it showed a negligible decrease of 3.4 nm in size (Figure 3D). Thus, these results showed that the H-CeO_2-PEG possessed excellent stability.

Excellent biocompatibility and no obvious toxicity are crucial for any applications in nanomedicine. Therefore, the cytotoxicity of H-CeO_2-PEG was studied in several types of cells. Firstly, FITC-labelled H-CeO_2-PEG were incubated with HCT116 cancer cells and imaged at different time points. As observed in Figure 3E, the FITC-labelled H-CeO_2-PEG showed a rapid cellular uptake. Subsequently, the H-CeO_2-PEG was incubated with NCM-460, HCT116 and SW480 cells at different concentrations (0, 5, 10, 25, 50, 100, and 125 μg/mL) for 24 h and 48 h. Then, the cell counting kit-8 (CCK-8) assays were performed to monitor the relative cytotoxicity, as shown in Figures 3F and G, no significant decrease in cellular viability was observed, indicating the ignorable cytotoxicity of H-CeO_2-PEG NPs. Therefore, these results exhibited the excellent physiological stability and biocompatibility of H-CeO_2-PEG and were capable of medical treatment application.

Effect of H-CeO_2-PEG on ROS in vitro

Previous studies have suggested that ROS could mediate the switch that regulates pro- or anti-inflammatory processes to determine the progression of various diseases.[36–38] Therefore, the effect of H-CeO_2-PEG on ROS scavenging in a hydroxyl radical-generating TiO_2/UV system was explored in vitro. As shown in Figure 4A, the BMPO/•OH signal had the strongest intensity on the TiO_2/UV system without H-CeO_2-PEG (control group, 0 μm/mL) and the concentration of H-CeO_2-PEG increased from 0 to 10 μm/mL, the intensity of BMPO/$^{\bullet}$OH signal decreased sharply that decreasing to 42% of that in the control group. And the intensity of BMPO/$^{\bullet}$OH signal decreased slowly and gradually when the concentration of H-CeO_2-PEG was further increased from 10 μg/mL to 50 μg/mL, when the H-CeO_2-PEG concentration increased to 50 μg/mL, the intensity of signal was only 12.6% of that in the control group, which indicated that H-CeO_2-PEG NPs possessed excellent ability to scavenge $^{\bullet}$OH. Furthermore, the POD-like activity of H-CeO_2-PEG was investigated by using TMB, a natural POD substrate where the POD is an ROS scavenger. The absorbance of TMB at 650 nm increased rapidly and significantly from 0 to 0.9 within 12 min after being treated with H-CeO_2-PEG NPs, indicating that H-CeO_2-PEG possessed POD-like activity (Figure 4B). At the same time, excessive generation of ROS contributes to the formation of superoxide radicals ($^{\bullet}$OOH), which are poisonous to cells, and the effect of H-CeO_2-PEG on $^{\bullet}$OOH was also evaluated in a xanthine/xanthine oxidase

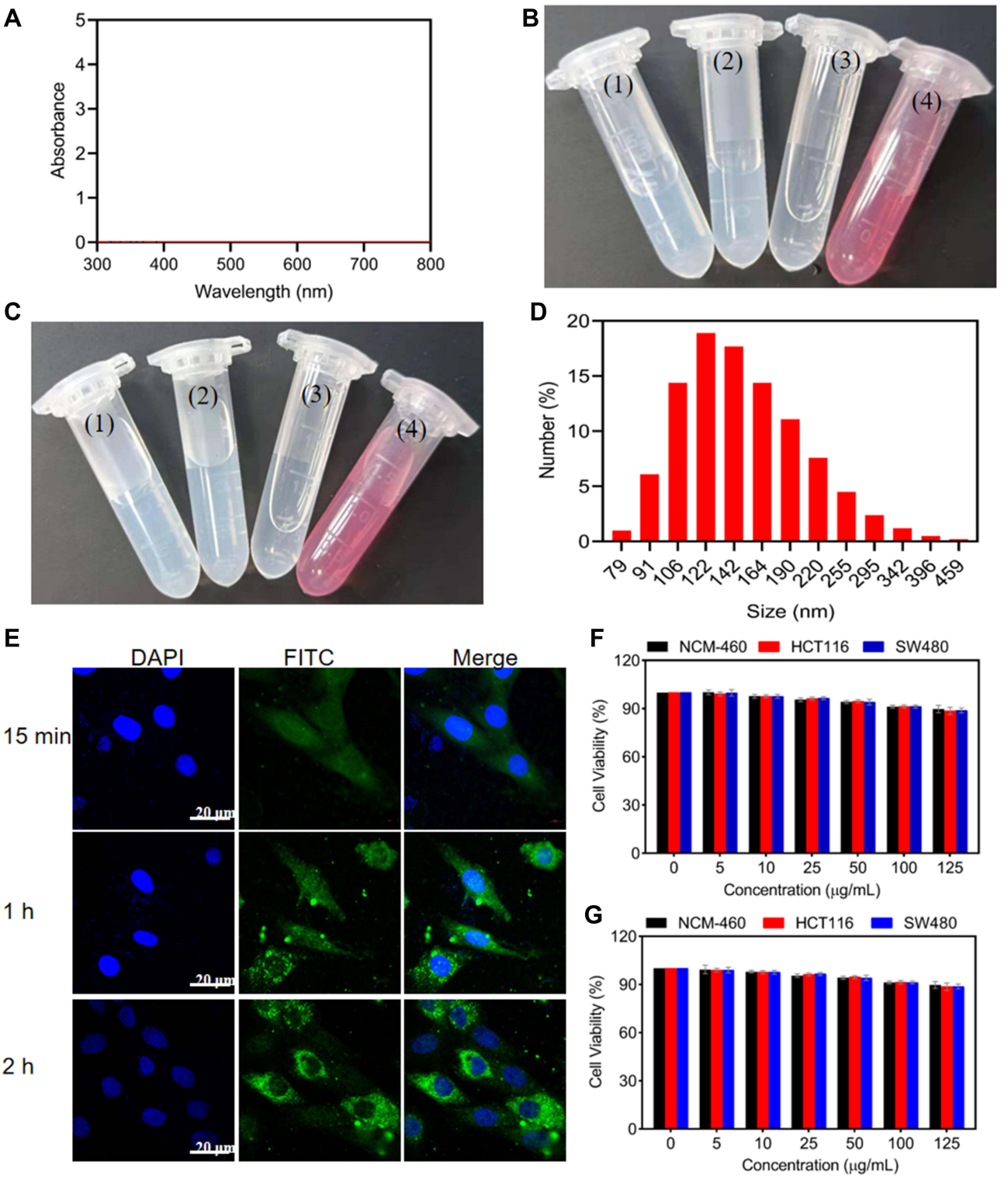

Figure 3 Stability and cytotoxicity of H-CeO_2-PEG. (**A**) Absorbance spectra of H-CeO_2-PEG. (**B**) Representative images of H-CeO_2-PEG in different solution, (1) ddH_2O, (2) PBS, (3) Ethanol, (4) DMEM culture. (**C**) Representative images of H-CeO_2-PEG dispersed in different solution for 7 days, (1) ddH_2O, (2) PBS, (3) Ethanol, (4) DMEM culture. (**D**) The particle size of H-CeO_2-PEG dispersed in ddH_2O for 7 days was analyzed by DLS analysis. (**E**) Representative cell uptake images of FITC-labelled H-CeO_2-PEG at different time. (**F**) Relative viability of various types of cells after incubation with different concentrations of H-CeO_2-PEG for 24 h; (**G**) Relative viability of various types of cells after incubation with different concentrations of H-CeO_2-PEG for 48 h.

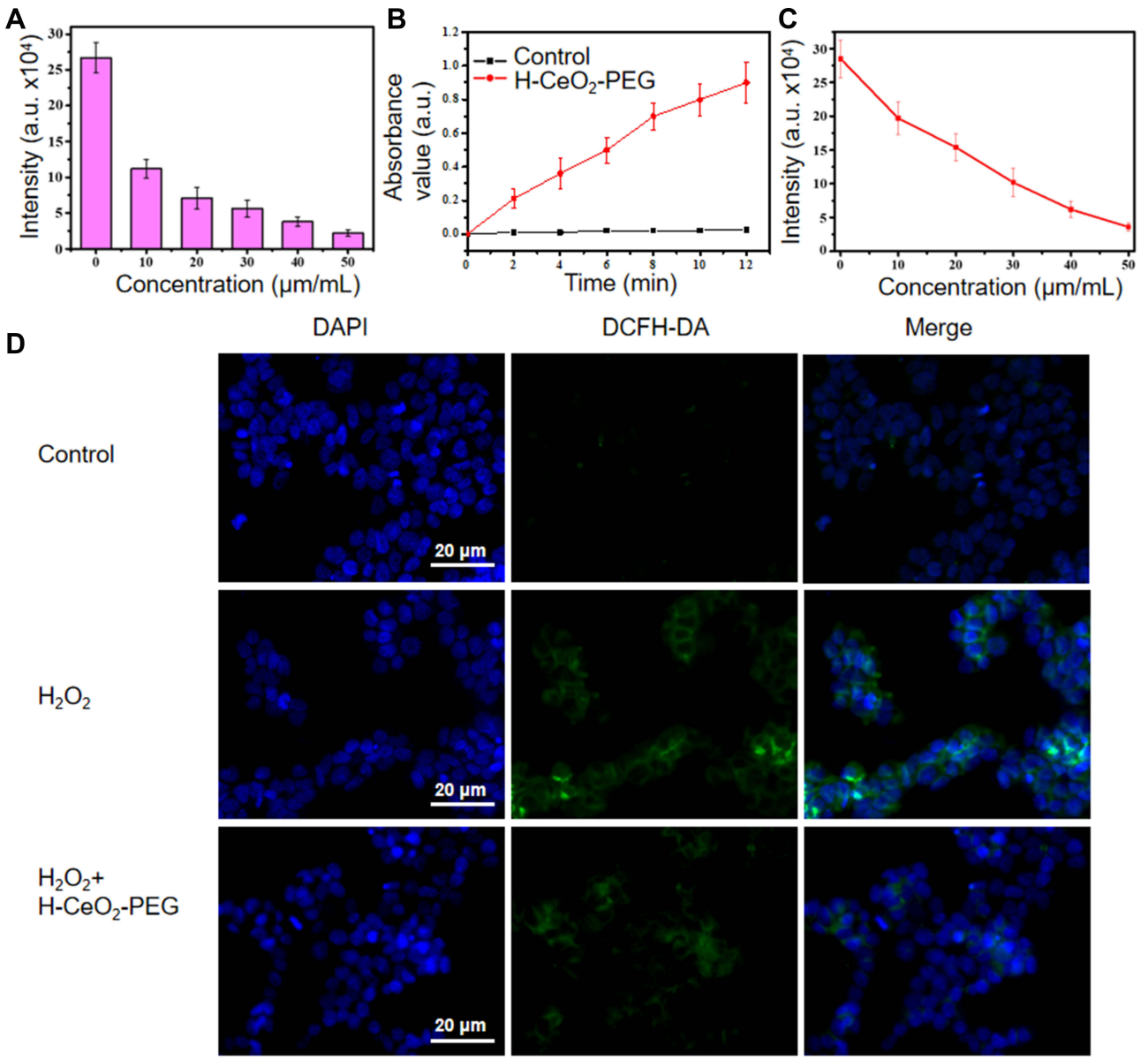

Figure 4 Evaluation of ROS scavenging in vitro. (**A**) Effect of H-CeO_2-PEG on •OH generated by a TiO_2/UV system. The signal intensities of the second line in the BMPO/•OH spectrum is presented. (**B**) POD-like activity of H-CeO_2-PEG. (**C**) Effect of H-CeO_2-PEG on •OOH produced by the xanthine/xanthine oxidase system. (**D**) CLSM images of ROS scavenging by H-CeO_2-PEG in HCT116 cells via DCFH-DA probe.

system. As shown in Figure 4C, the BMPO/$^{\bullet}$OOH signal intensity decreases dramatically in H-CeO_2-PEG concentration-dependent manner, suggesting that H-CeO_2-PEG exerts SOD-like enzyme activity to scavenge $^{\bullet}$OOH. Finally, we examined the scavenging capability of ROS of H-CeO_2-PEG in HCT116 cancer cells. The cancer cells were incubated with 100 μM H_2O_2 for generating excessive ROS within cells. As shown in Figure 4D, the results of DCFH-DA probe staining revealed that H_2O_2 induced high generation efficacy of ROS, and H-CeO_2-PEG NPs scavenged the ROS effectively. These results suggested that H-CeO_2-PEG possessed good ROS scavenging capability.

Therapeutic Effect of H-CeO_2-PEG in DSS-Induced Colitis Mice

Based on the excellent POD- and SOD-like activity of H-CeO_2-PEG NPs, it was speculated that H-CeO_2-PEG could scavenge ROS- in inflammation-related diseases. Moreover, nanoparticles can accumulate in the site of inflammation from the blood via endothelial pathways due to their recognized ability to enhance permeability

and retention effect (EPR) and absorption by infiltrating inflammatory cells (Figure 5B),[39] EPR helps significantly improve targeting capability and therapeutic effects. Hence, we first investigated whether H-CeO_2-PEG could accumulate in the inflamed colon and further observed its therapeutic effect on DSS-induced colitis mice (Figure 5A). A DSS-induced colitis model was constructed by providing a 3% (wt%) solution of DSS for drinking instead of water for one week. The mice (n = 3) were injected with H-CeO_2-PEG NPs (20 mg/kg) intravenously, and the main organs (heart, liver, spleen, lung and kidney) and colon were collected in different time (12 h, 1 day and 7 day,) and analysed the concentration of Ce using inductively coupled plasma atomic emission spectrometry (ICP-AES) to evaluate the colitis accumulation and biodistribution of NPs. As shown in Figure 5C, the concentration of Ce was 13.26 μg/g at 12 h and 19.42 μg/g at 1 day post-injection, suggesting colitis effectively accumulation of the H-CeO_2-PEG NPs. And the Ce concentrations were found not only in the colitis tissues, but also in other organs, such as the liver and spleen. Meantime, it was 10.63 μg/g in colon at 7 days post-injection, which was lower than the concentration at 12 h and 1 day, implied that the Ce concentrations in colitis tissues reduced gradually, as observed for other organs; however, the reduction rate in colitis tissues was lower than that in other organs. Then, meantime, the mice fed with DSS to construct colitis were divided into two groups, where the healthy mice were set as control group. PBS and H-CeO_2-PEG NPs (20 mg/kg) were injected intravenously at 1, 3, 5 and 7 days, respectively, and the therapeutic effects was evaluated on days 9 to 21 days, including the change of body weight, disease activity index (DAI), colon length, and haematochezia rate. As shown in Figure 5D, the DSS-feeding to construct the colitis model of mice induced the loss of body weight, which showed the establishment of colitis. Then, we evaluated the DAI to access the situation of colitis, we found that when treated with H-CeO_2-PEG NPs, it alleviated the dramatic weight loss, where the DAI in the DSS group was 3, and it was 0.3 and 1.7 in the control group and DSS + H-CeO_2-PEG group, implying that the H-CeO_2-PEG rescued the colitis induced by DSS (Figure 5E).[40] Moreover, the results of colon length measurement showed the severe inflammation in colons of colitis mice were shorter and severe bleeding, and treated with H-CeO_2-PEG NPs, it showed longer length of colon, bleeding, or abnormal stools compared to the mice that without treatment (Figures 5F and G). Similar to the body weight and DAI results, the haematochezia rate in the colitis group was greater than 80% compared to the control group, and the haematochezia rate after H-CeO_2-PEG treatment was significantly reduced to approximately 40% (Figure 5H), which also indicated the colitis occurrence induced by DSS and H-CeO_2-PEG decreased the haematochezia rate to about 50%, suggesting H-CeO_2-PEG alleviated the colitis. Meanwhile, the colons were also collected and applied histological analysis to observe the change of structure after different treatment. We observed that mice with colitis show severe destruction of mucosal areas, massive infiltration and severe colonic epithelial damage, and relief of damage after treated with H-CeO_2-PEG displayed minor damage and infiltration in the mucosa or muscle, and showed a negligible damage in the control group (Figures 5I and J). Furthermore, the colons were collected after different treatment and stained with ROS probe to evaluate the ROS scavenging capability of H-CeO_2-PEG in vivo. As shown in Figure 5K, the mice treated with H-CeO_2-PEG leaded to an obvious reduction of ROS compared to the DSS treated mice, suggesting the excellent therapeutic effect in colitis via scavenging ROS effectively. All these evidences demonstrate the excellent therapeutic effect of H-CeO_2-PEG on DSS-induced colitis.

Then, we further confirmed the therapeutic effects of H-CeO_2-PEG on DSS-induced colitis by western blotting analysis, which was performed to detect expression changes in colitis-related proteins (claudin-1, ZO1, Occu, and ZO2). As shown in Figures 6A and B, the protein expression of claudin-1, ZO1, Occu and ZO2 was significantly upregulated in the colonic tissues of DSS-induced colitis mice compared with those of control mice, whereas H-CeO_2-PEG treatment regulated the expression of these proteins inhibited compared to the expression in healthy mice. On the other hand, the levels of proinflammatory cytokines, including IL-6, TNF-α, IL-1β, and IL-18, in the colitic colon were further determined using qPCR analysis and quantification with commercial ELISA kits to examine the damage of colitis further. Compared to the mice in control group, the levels of IL-6, TNF-α, IL-1β, and IL-18 fed with DSS were significantly increased, whereas treated with H-CeO_2-PEG NPs decreased the expression of IL-6, TNF-α, IL-1β, and IL-18 in mRNA and protein level that induced with DSS (Figures 6C and D). These results demonstrate that H-CeO_2-PEG possessed an excellent ability to alleviate colitis.

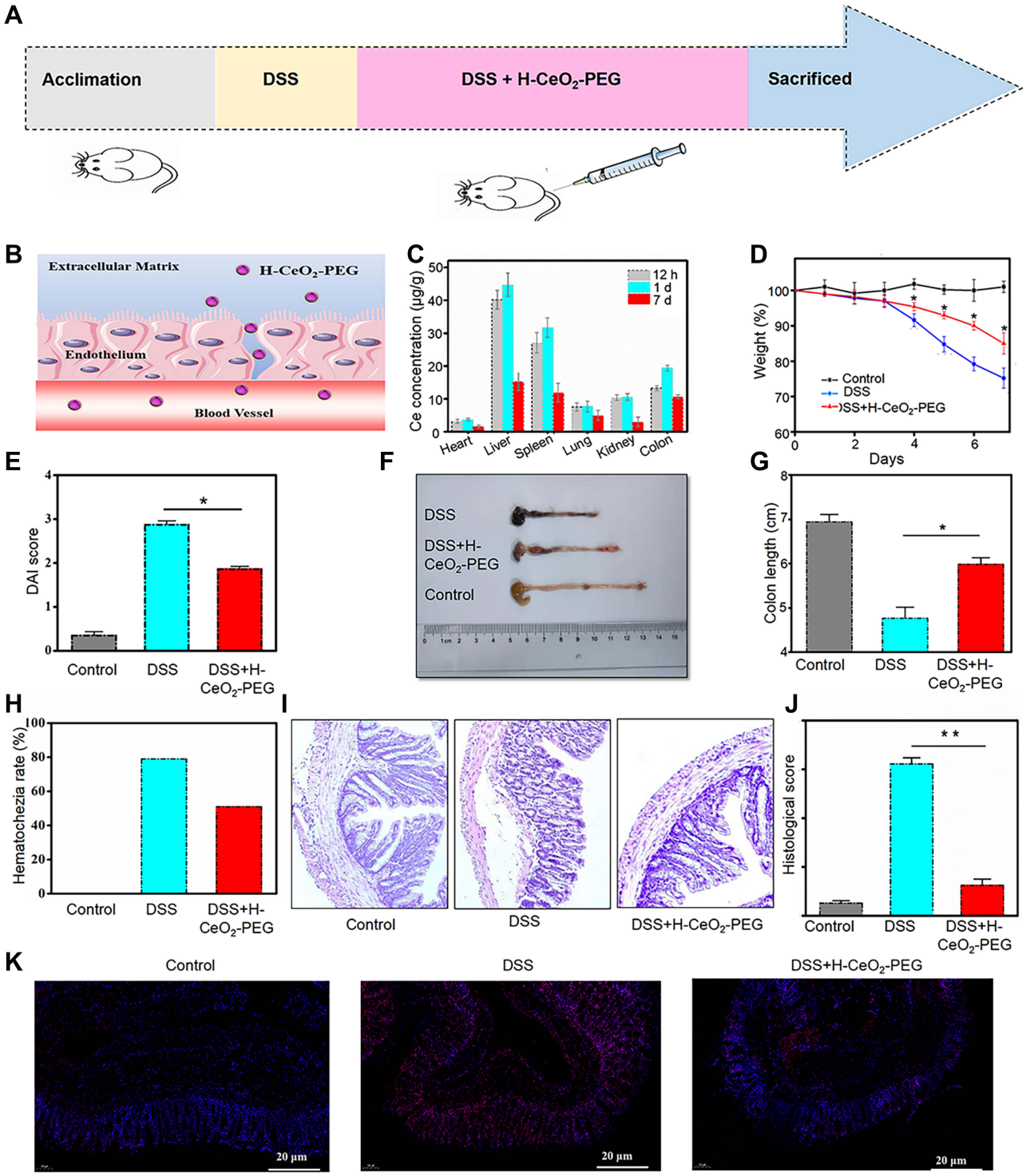

Figure 5 Evaluation of therapeutic effects of H-CeO_2-PEG in vivo. (**A**) Overall experimental procedure. Mice were provided normal water or water containing 3% DSS for 7 days. On days 1, 3, 5, and 7, the mice were treated with H-CeO_2-PEG or normal saline. (**B**) H-CeO_2-PEG was intravenously administered to DSS-induced colitis model mice to target the inflamed colon from the endothelium via a mechanism mediated by size. (**C**) Ce concentrations at different time intervals of 12 h,1 day and 7 days after intravenously injection. (**D**) The weight of the mice treated with H-CeO_2-PEG or normal saline. (**E**) DAI scores of the mice treated with H-CeO_2-PEG or normal saline. (**F** and **G**) Colon lengths and corresponding images of colons from each group. (**H**) Haematochezia rate of the mice treated with H-CeO_2-PEG or normal saline. DAI, disease activity index. (**I**) H&E-stained colon sections from each group. (**J**) Histological scores from (**I**). (**K**) Representative images of the ROS staining (red: ROS, blue: DAPI). *P< 0.05; **P< 0.01. A P value less than 0.05 was defined as statistically significance.

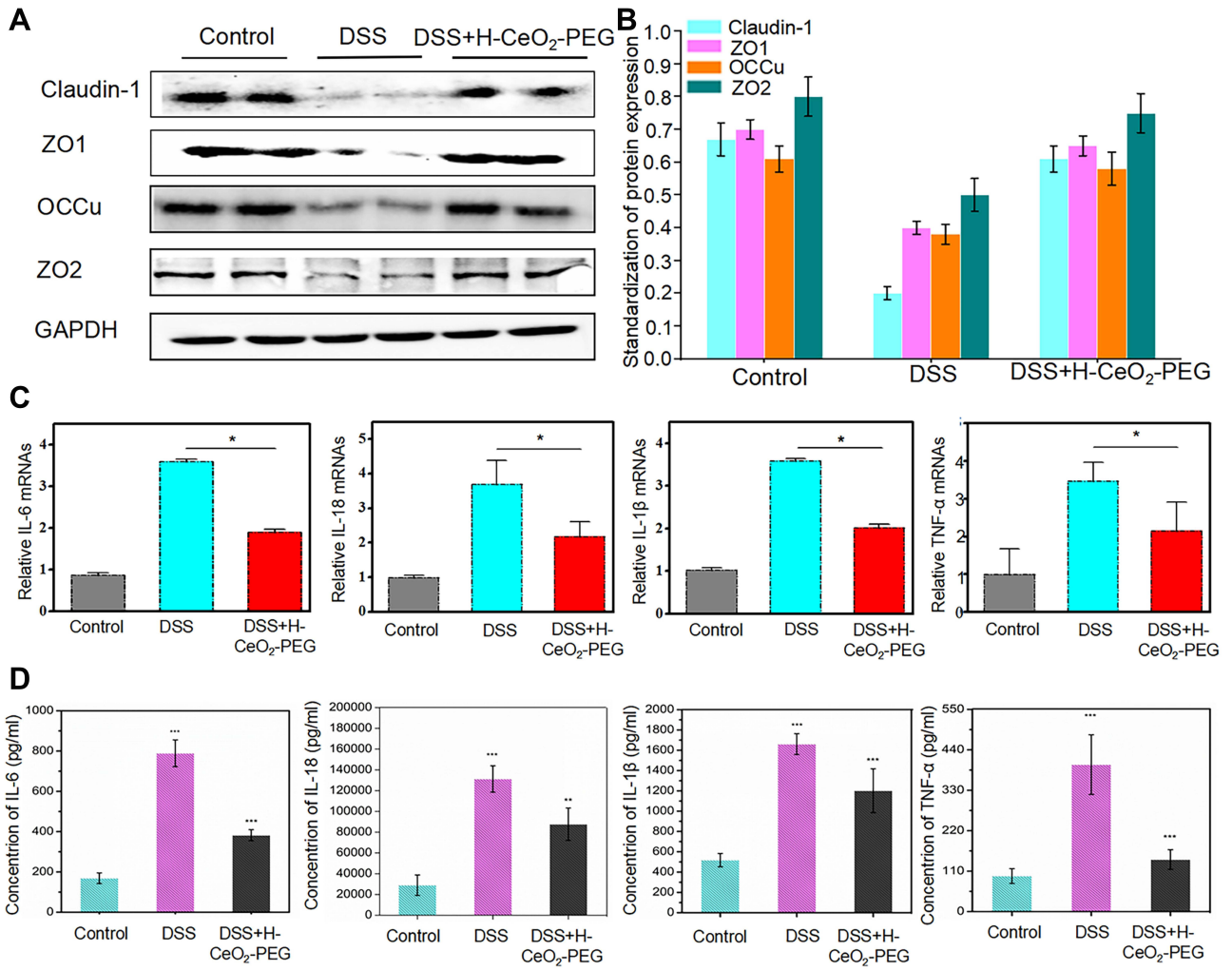

Figure 6 Evaluation of therapeutic effects of H-CeO_2-PEG. (**A** and **B**) Western blotting analysis and quantification of claudin-1, ZO1, Occu and ZO2 protein expression in colitis tissue from each group. (**C**) qPCR analysis of IL-6, TNF-α, IL-1β, and IL-18 mRNA expression in colitis tissue from each group. (**D**) Elisa quantification of IL-6, TNF-α, IL-1β, and IL-18 mRNA expression in colitis tissue from each group. *P< 0.05; **P< 0.01; **P< 0.001. A P value less than 0.05 was defined as statistically significance.

Molecular Mechanism of H-CeO_2-PEG in the Treatment of Colitis

Previous research has shown that DSS-induced colitis is regulated by different signalling pathways.[41–45] On the other hand, many studies have reported that CeO_2 can activate the MAPK signalling pathway to control the growth of new blood and the degranulation process and induce cytotoxicity.[46–48] For instance, Bao and colleagues' reported that baicalein stabilized CeO_2 NPs hindered the pro-inflammatory cytokine release and blocked the MAPK signalling pathway in rotenone-stimulated PD rat models.[49] In other studies, many reports revealed that the ROS is tightly associated with the MAPK signalling pathway. For instance, Akira Murakami et al revealed that DSS induces the activation of p38 MAPK via ROS generation, and combined the activation of ERK1/2 to enhance the release of IL-1β.[50] In another study, Ho Kim and colleagues' study showed that the activation of p38 MAPK signalling pathway with Toxin A in neuronal cells is dependent on ROS production.[51] Hence, we further investigated whether H-CeO_2-PEG alleviate colitis via inhibiting the activation of MAPK signalling pathway. The results of western blotting analysis showed that the levels of p-ERK1/2 (phosphorylated ERK1/2), p-JNK (phosphorylated JNK), p-p38 (phosphorylated p38) and p-c-Jun (phosphorylated c-Jun) were markedly increased with DSS induction (Figures 7A and B), and as we expected, the levels of p-ERK1/2, p-JNK, p-p38 and p-c-Jun in colonic tissue were decreased significantly after treated with H-CeO_2-PEG in colitis and compared with the control group (Figures 7A and B), suggesting that H-CeO_2-PEG administration could repair the DSS-

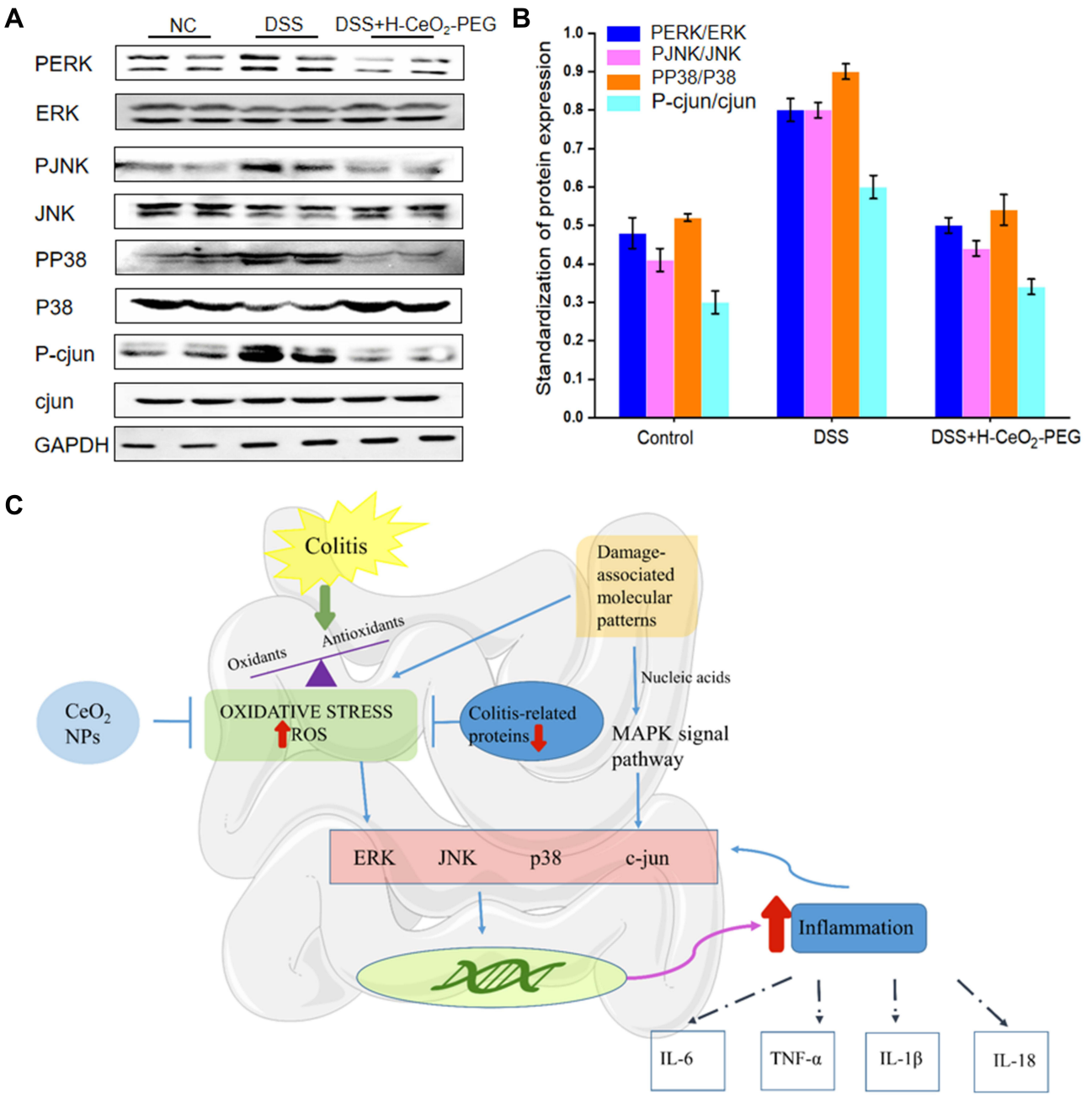

Figure 7 Molecular mechanism underlying the colitis relief cell death after treatment with H-CeO_2-PEG. (**A** and **B**) Western blotting and quantification analysis of ERK, JNK, p38 and c-Jun protein expression and phosphorylated ERK, JNK, p38 and c-Jun protein expression levels in colitis tissue from the control group, DSS-induced colitis group, and H-CeO_2-PEG-treated DSS-induced colitis group. (**C**) Schematic illustration of the involved molecular pathway.

induced damage via inhibiting the MAPK signalling pathway (Figure 7C).

In vivo Toxicity of H-CeO_2-PEG

Biosafety is a crucial index for nanomaterial-based therapy. The potential toxicity of H-CeO_2-PEG was investigated systematically in vivo. To explore the potential toxicity of H-CeO_2-PEG in vivo, blood and organs (heart, liver, spleen, lung kidney and colon) of healthy mice without DSS-treatment were administered with H-CeO_2-PEG and biosafety evaluation were latterly studied. The following standard hematological markers were assessed, including white blood cells (WBC), red blood cell (RBC), mean corpuscular volume (MCV), mean corpuscular hemoglobin (MCH), and mean corpuscular hemoglobin concentration (MCHC) (Figure 8A). There

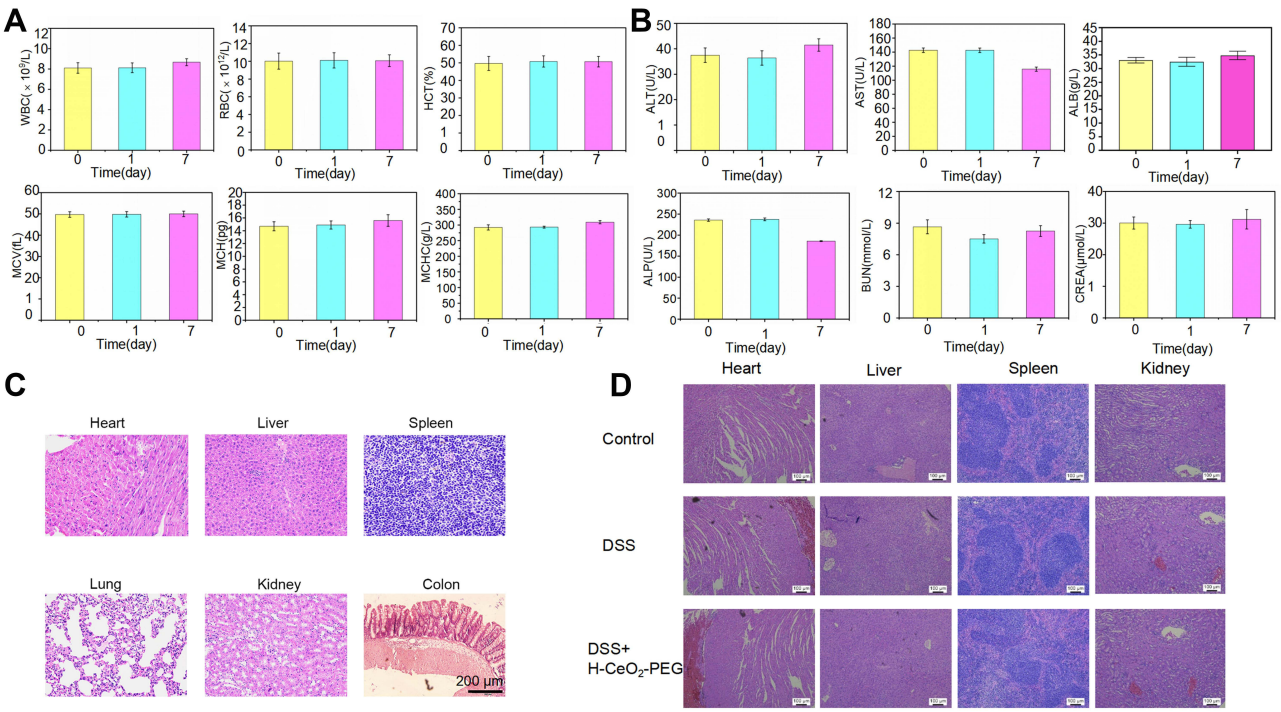

Figure 8 In vivo toxicology evaluation of H-CeO_2-PEG. (**A**) Hematological indicators. (**B**) Blood biochemistry indicators. (**C**) H&E stained images of tissue from the heart, liver, spleen, lung, kidneys and colon from the healthy mice. (**D**) H&E stained images of organs from the mice after different treatment.

were no significant differences were observed in these parameters, suggesting that the H-CeO_2-PEG did not cause any distinct effects in treated mice. And the following blood biochemistry parameters were also examined, including alanine transaminase (ALT), aspartate transaminase (AST), albumin (ALB), alkaline phosphatase (ALP), blood urea nitrogen (BUN), creatinine (CREA). Again, there was no significant difference among these values in treated mice (Figure 8B). Furthermore, histopathology analysis of the main organs (heart, liver, spleen, kidney and colon) demonstrated no observable impairments occurred with H-CeO_2-PEG treatment (Figure 8C). Furthermore, we also examined the possible toxicity of H-CeO_2-PEG to the main organs (heart, liver, spleen and kidney) in the colitis model mice using H&E staining, no obvious damages were observed (Figure 8D). These results confirmed that negligible toxicity was observed after H-CeO_2-PEG administration, demonstrating the excellent biocompatibility and biosafety of H-CeO_2-PEG.

Discussion and Conclusions

In summary, we successfully prepared highly monodispersed hollow CeO_2 with good stability and it was capable of being used as a nanozyme for colitis treatment. It was proved that the H-CeO_2-PEG was an effective ROS scavenger that converted harmful ROS, including •OH, H_2O_2, and •OOH, to H_2O and O_2 through its nanozyme activity, alleviating oxidative stress and showing a certain therapeutic effect on colitis. The result of the molecular mechanism experiment demonstrated that H-CeO_2-PEG inhibited the activation of ERK1/2/JNK/p38/c-Jun to decrease inflammation in DSS-induced colitis. This work provides a new point that H-CeO_2-PEG could be regarded as a potential alternative agent for the treatment of colitis.

Acknowledgment

This work was supported by the Natural Science Foundation of Shandong Province (No. ZR2012HL20), the Medical and Health Technology Development Program of Shandong Province (No. 2015WS0221) and the Shanghai Natural Science Foundation of China (No. SKW1921), Shandong Provincial Integrated Traditional Chinese and Western Medicine Special Disease Prevention Project (No. SDPR-2020-0230007), the Science, Technology & Innovation Commission of Shenzhen Municipality (Nos. JCYJ201 90807144605514), the Scientific Research Program of Shanghai Science and Technology Commission (SKW1 921), the Clinical Research and Cultivation Project of Shanghai Tongji Hospital (ITJ(ZD)1802).

Disclosure

All authors declared no conflicts of interest.

References

1. Tabas I, Glass CK. Anti-Inflammatory therapy in chronic disease: challenges and opportunities. *Science*. 2013;339(6116):166–172. doi:10.1126/science.1230720
2. Coussens LM, Werb Z. Inflammation and cancer. *Nature*. 2002;420 (6917):860–867. doi:10.1038/nature01322
3. Mantovani A, Allavena P, Sica A, Balkwill F. Cancer-related inflammation. *Nature*. 2008;454(7203):436–444. doi:10.1038/nature 07205
4. Bishayee A. The role of inflammation in liver cancer. *Inflammation Cancer*. 2014;816:401–435.
5. Chapman TP, Gomes CF, Louis E, Colombel JF, Satsangi J. De-escalation of immunomodulator and biological therapy in inflammatory bowel disease. *Lancet Gastroenterol Hepatol*. 2020;5(1):63–79. doi:10.1016/S2468-1253(19)30186-4
6. Hoivik ML, Moum B, Solberg IC, et al. Health-related quality of life in patients with ulcerative colitis after a 10-year disease course: results from the IBSEN study. *Inflamm Bowel Dis*. 2012;18 (8):1540–1549. doi:10.1002/ibd.21863
7. Maloy KJ, Powrie F. Intestinal homeostasis and its breakdown in inflammatory bowel disease. *Nature*. 2011;474(7351):298–306. doi:10.1038/nature10208
8. Guo HT, Callaway JB, Ting JPY. Inflammasomes: mechanism of action, role in disease, and therapeutics. *Nat Med*. 2015;21 (7):677–687. doi:10.1038/nm.3893
9. Nordberg J, Arner ESJ. Reactive oxygen species, antioxidants, and the mammalian thioredoxin system. *Free Radical Bio Med*. 2001;31 (11):1287–1312.
10. Ohsawa I, Ishikawa M, Takahashi K, et al. Hydrogen acts as a therapeutic antioxidant by selectively reducing cytotoxic oxygen radicals. *Nat Med*. 2007;13(6):688–694. doi:10.1038/nm1577
11. Mittal M, Siddiqui MR, Tran K, Reddy SP, Malik AB. Reactive oxygen species in inflammation and tissue injury. *Antioxid Redox Signal*. 2014;20(7):1126–1167. doi:10.1089/ars.2012.5149
12. Valko M, Leibfritz D, Moncol J, Cronin MTD, Mazur M, Telser J. Free radicals and antioxidants in normal physiological functions and human disease. *Int J Biochem Cell B*. 2007;39(1):44–84. doi:10.1016/j.biocel.2006.07.001
13. Ananthakrishnan AN. Epidemiology and risk factors for IBD. *Nat Rev Gastro Hepat*. 2015;12(4):205–217. doi:10.1038/nrgastro.2015.34
14. Chen ZJ, Vong CT, Gao CF, et al. Bilirubin nanomedicines for the treatment of reactive oxygen species (ROS)-Mediated Diseases. *Mol Pharm*. 2020;17(7):2260–2274. doi:10.1021/acs.molpharmaceut.0c00337
15. Wang LY, Zhu BH, Deng YT, et al. Biocatalytic and Antioxidant Nanostructures for ROS Scavenging and Biotherapeutics. *Adv Funct Mater*. 2021:2101804.
16. Wu LH, Cai XJ, Zhu HF, et al. PDT-Driven Highly Efficient Intracellular Delivery and Controlled Release of CO in Combination with Sufficient Singlet Oxygen Production for Synergistic Anticancer Therapy. *Adv Funct Mater*. 2018;28:41. doi:10.1002/adfm.201804324
17. Yu W, Liu T, Zhang M, et al. O2 economizer for inhibiting cell respiration to combat the hypoxia obstacle in tumor treatments. *Acs Nano*. 2019;13(2):1784–1794.
18. Yao C, Wang WX, Wang PY, Zhao MY, Li XM, Zhang F. Near-infrared upconversion mesoporous cerium oxide hollow biophotocatalyst for concurrent pH-/H2 O2-Responsive O2-Evolving Synergetic Cancer Therapy. *Adv Mater*. 2018;30(7):1704833. doi:10.1002/adma.201704833
19. Wachsmann P, Lamprecht A. Polymeric nanoparticles for the selective therapy of inflammatory bowel disease. *Method Enzymol*. 2012;508:377.
20. Valesini G, Gerardi MC, Iannuccelli C, Pacucci VA, Pendolino M, Shoenfeld Y. Citrullination and autoimmunity. *Autoimmun Rev*. 2015;14(6):490–497. doi:10.1016/j.autrev.2015.01.013
21. Li FY, Zhu SX, Wang ZP, Wang H, Zhao Y, Chen GP. Consumption of hydrogen-rich water protects against ferric nitrilotriacetate-induced nephrotoxicity and early tumor promotional events in rats. *Food Chem Toxicol*. 2013;61:248–254. doi:10.1016/j.fct.2013.10.004
22. Zhang W, Hu SL, Yin JJ, et al. Prussian blue nanoparticles as multi-enzyme mimetics and reactive oxygen species scavengers. *J Am Chem Soc*. 2016;138(18):5860–5865. doi:10.1021/jacs.5b12070
23. Abdelmegid AM, Abdo FK, Ahmed FE, Kattaia AAA. Therapeutic effect of gold nanoparticles on DSS-induced ulcerative colitis in mice with reference to interleukin-17 expression. *Sci Rep*. 2019;1:9.
24. Zhu SQ, Zeng MY, Feng GX, Wu HH. Platinum nanoparticles as a therapeutic agent against dextran sodium sulfate-induced colitis in mice. *Int J Nanomedicine*. 2019;14:8361–8378. doi:10.2147/IJN.S210655
25. Ruiz PA, Moron B, Becker HM, et al. Titanium dioxide nanoparticles exacerbate DSS-induced colitis: role of the NLRP3 inflammasome. *Gut*. 2017;66(7):1216–1224. doi:10.1136/gutjnl-2015-310297
26. Nishiguchi A, Taguchi T. Oligoethyleneimine-conjugated hyaluronic acid modulates inflammatory responses and enhances therapeutic efficacy for ulcerative colitis. *Adv Funct Mater*. 2021;31:30. doi:10.1002/adfm.202100548
27. Hirst SM, Karakoti AS, Tyler RD, Sriranganathan N, Seal S, Reilly CM. Anti-inflammatory Properties of Cerium Oxide Nanoparticles. *Small*. 2009;5(24):2848–2856. doi:10.1002/smll.200901048
28. Demokritou P, Gass S, Pyrgiotakis G, et al. An in vivo and in vitro toxicological characterisation of realistic nanoscale CeO2 inhalation exposures. *Nanotoxicology*. 2013;7(8):1338–1350. doi:10.3109/17435390.2012.739665
29. Celardo I, Pedersen JZ, Traversa E, Ghibelli L. Pharmacological potential of cerium oxide nanoparticles. *Nanoscale*. 2011;3 (4):1411–1420. doi:10.1039/c0nr00875c
30. Nemmar A, Al-Salam S, Beegam S, Yuvaraju P, Ali BH. Aortic Oxidative Stress, Inflammation and DNA Damage Following Pulmonary Exposure to Cerium Oxide Nanoparticles in a Rat Model of Vascular Injury. *Biomolecules*. 2019;9:8. doi:10.3390/biom9080376
31. Vassie JA, Whitelock JM, Lord MS. Endocytosis of cerium oxide nanoparticles and modulation of reactive oxygen species in human ovarian and colon cancer cells. *Acta Biomater*. 2017;50:127–141. doi:10.1016/j.actbio.2016.12.010
32. Xu C, Qu XG. Cerium oxide nanoparticle: a remarkably versatile rare earth nanomaterial for biological applications. *npg Asia Mater*. 2014;2:6.
33. Montini T, Melchionna M, Monai M, Fornasiero P. Fundamentals and Catalytic Applications of CeO2-Based Materials. *Chem Rev*. 2016;116(10):5987–6041. doi:10.1021/acs.chemrev.5b00603
34. Asgharzadeh F, Hashemzadeh A, Rahmani F, et al. Cerium oxide nanoparticles acts as a novel therapeutic agent for ulcerative colitis through anti-oxidative mechanism. *Life Sci*. 2021;278:119500. doi:10.1016/j.lfs.2021.119500
35. Zhao S, Li YX, Liu QY, et al. An Orally Administered CeO2 @Montmorillonite Nanozyme Targets Inflammation for Inflammatory Bowel Disease Therapy. *Adv Funct Mater*. 2020;30 (45):2004692. doi:10.1002/adfm.202004692
36. Nathan C, Ding AH. Nonresolving Inflammation. *Cell*. 2010;140 (6):871–882. doi:10.1016/j.cell.2010.02.029
37. Nian M, Lee P, Khaper N, Liu P. Inflammatory cytokines and post-myocardial infarction remodeling. *Circ Res*. 2004;94(12):1543–1553. doi:10.1161/01.RES.0000130526.20854.fa
38. Kunsch C, Medford RM. Oxidative stress as a regulator of gene expression in the vasculature. *Circ Res*. 1999;85(8):753–766. doi:10.1161/01.RES.85.8.753

39. Torchilin V. Tumor delivery of macromolecular drugs based on the EPR effect. *Adv Drug Deliv Rev*. 2011;63(3):131–135. doi:10.1016/j.addr.2010.03.011
40. Zhao JL, Cai XJ, Gao W, et al. Prussian Blue Nanozyme with Multienzyme Activity Reduces Colitis in Mice. *ACS Appl Mater Interfaces*. 2018;10(31):26108–26117. doi:10.1021/acsami.8b10345
41. Elinav E, Strowig T, Kau AL, et al. NLRP6 Inflammasome Regulates colonic microbial ecology and risk for colitis. *Cell*. 2011;145(5):745–757. doi:10.1016/j.cell.2011.04.022
42. Gadaleta RM, van Erpecum KJ, Oldenburg B, et al. Farnesoid X receptor activation inhibits inflammation and preserves the intestinal barrier in inflammatory bowel disease. *Gut*. 2011;60(4):463–472. doi:10.1136/gut.2010.212159
43. Ghia JE, Blennerhassett P, Kumar-Ondiveeran H, Verdu EF, Collins SM. The vagus nerve: a tonic inhibitory influence associated with inflammatory bowel disease in a murine model. *Gastroenterology*. 2006;131(4):1122–1130. doi:10.1053/j.gastro.2006.08.016
44. Chami B, San Gabriel PT, Kum-Jew S, et al. The nitroxide 4-methoxy-tempo inhibits the pathogenesis of dextran sodium sulfate-stimulated experimental colitis. *Redox Biol*. 2020;28:101333.
45. Ren YJ, Yue B, Ren GY, et al. Activation of PXR by alantolactone ameliorates DSS-induced experimental colitis via suppressing NF-kappa B signaling pathway. *Sci Rep*. 2019;9:1–2.
46. Cheng GL, Guo W, Han L, et al. Cerium oxide nanoparticles induce cytotoxicity in human hepatoma SMMC-7721 cells via oxidative stress and the activation of MAPK signaling pathways. *Toxicology in Vitro*. 2013;27(3):1082–1088. doi:10.1016/j.tiv.2013.02.005
47. Nethi SK, Nanda HS, Steele TWJ, Patra CR. Functionalized nanoceria exhibit improved angiogenic properties. *J Mater Chem B*. 2017;5(47):9371–9383. doi:10.1039/C7TB01957B
48. Babin K, Antoine F, Goncalves DM, Girard D. TiO2, CeO2 and ZnO nanoparticles and modulation of the degranulation process in human neutrophils. *Toxicol Lett*. 2013;221(1):57–63. doi:10.1016/j.toxlet.2013.05.010
49. Zhang Z, Zhong M, Wang J, Xia DJ, Bao JS. Synthesis of Baicalein Modified Cerium Oxide Nanoparticles for Inhibitory Activation of NF-kappa B and Mitogen-Activated Protein Kinase Signals in Rotenone-Induced Parkinsonian Rats. *Sci Adv Mater*. 2020;12(1):93–100. doi:10.1166/sam.2020.3594
50. Kwon KH, Ohigashi H, Murakami A. Dextran sulfate sodium enhances interleukin-1 beta release via activation of p38 MAPK and ERK1/2 pathways in murine peritoneal macrophages. *Life Sci*. 2007;81(5):362–371. doi:10.1016/j.lfs.2007.05.022
51. Zhang P, Hong J, Yoon IN, Kang JK, Hwang JS, Kim H. Clostridium difficile Toxin A Induces Reactive Oxygen Species Production and p38 MAPK Activation to Exert Cellular Toxicity in Neuronal Cells. *J Microbiol Biotechnol*. 2017;27(6):1163–1170. doi:10.4014/jmb.1702.02041